Entanglement Growth and Minimal Membranes in $(d+1)$ Random Unitary Circuits

Piotr Sierant,[1] Marco Schirò,[2] Maciej Lewenstein,[1] and Xhek Turkeshi[2,3]

[1]*ICFO-Institut de Ciències Fotòniques, The Barcelona Institute of Science and Technology, Av. Carl Friedrich Gauss 3, 08860 Castelldefels (Barcelona), Spain*

[2]*JEIP, UAR 3573 CNRS, Collège de France, PSL Research University, 11 Place Marcelin Berthelot, 75321 Paris Cedex 05, France*

[3]*Institut für Theoretische Physik, Universität zu Köln, Zülpicher Strasse 77, 50937 Köln, Germany*

(Received 30 June 2023; revised 5 September 2023; accepted 9 November 2023; published 8 December 2023)

Understanding the nature of entanglement growth in many-body systems is one of the fundamental questions in quantum physics. Here, we study this problem by characterizing the entanglement fluctuations and distribution of a $(d+1)$-dimensional qubit lattice evolved under a random unitary circuit. Focusing on Clifford gates, we perform extensive numerical simulations of random circuits in $1 \le d \le 4$ dimensions. Our findings demonstrate that properties of growth of bipartite entanglement entropy are characterized by the roughening exponents of a d-dimensional membrane in a $(d+1)$-dimensional elastic medium.

DOI: 10.1103/PhysRevLett.131.230403

Characterizing entanglement evolution in many-body quantum systems is an essential problem in statistical mechanics, condensed matter theory, and high-energy physics [1–3]. For instance, it has profound implications for quantum thermalization [4–11] and its breakdown in disordered systems [12–22]. At the same time, it provides new perspectives on quantum chaos arising in semiclassical and long-range systems [23–27] or holographic models [28–35]. However, comprehending entanglement dynamics is of notorious difficulty due to the nonlocal nature of the quantum correlations. Insights into one-dimensional systems come from conformal field theory and integrability [36–46], exactly solvable dual-unitary dynamics [47–53], and extensive numerical investigations [54–61]. These results motivate the search for a phenomenological understanding of quantum information scrambling in generic many-body systems.

Because of their simple structure, random unitary circuits are ideal candidates for this purpose [62]. References [63–65] demonstrated that the evolution of entanglement entropy of $(1+1)D$ circuits maps, in suitable limits, to the properties of a line defect in a two-dimensional elastic medium. Those insights go beyond the leading-order contribution to the entanglement entropy growth and are reflected in structural aspects of entanglement propagation. A nontrivial verification of this fact is the Kardar-Parisi-Zhang (KPZ) universal growth of entanglement fluctuations in $(1+1)D$ Clifford and Haar random unitary circuits [63–65]. Inspired by these results, the authors of Ref. [63] conjectured that the structural aspects of the entanglement growth in generic $(d+1)$-dimensional systems correspond to a d-dimensional membrane in a $(d+1)$-dimensional elastic medium. The membrane, on a coarse-grained level, is fixed by the minimal cut of entanglement bonds across space-time, resulting, for random unitary circuits, in the entanglement growth being governed by exponents of an elastic manifold pinned by the disorder [66–69]. However, without any numerical and analytical results for $d > 1$, it remains unclear whether this minimal membrane picture (MMP) indeed provides insights into the structure of entanglement evolution in higher-dimensional systems.

This Letter answers this question affirmatively by investigating $(d+1)$-dimensional random Clifford circuits with $2 \le d \le 4$ comprising up to $N = 131\,072$ qubits. We

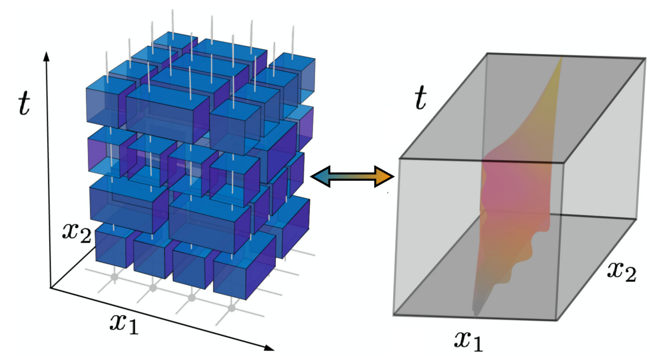

	Entanglement		Membrane		RG
$d+1$	θ	ζ	θ	ζ	ζ
2+1	0.861(6)	0.435(33)	0.84(3)	0.41(1)	0.423
3+1	1.401(9)	0.3(1)	1.45(4)	0.22(1)	0.211
4+1	2.000(5)	-	2	-	-

FIG. 1. Illustration: the entanglement growth in a $(d+1)$-dimensional random unitary circuit is conjectured to map to a problem of a d-dimensional membrane in a $(d+1)$-dimensional disordered medium. Table: summary of our results (Entanglement), comparison with random bond Ising model [70,71] (Membrane), and with the renormalization group [72–76] (RG). Exponents characterizing entanglement propagation under noisy unitary dynamics in $(d+1)$ dimensions confirm the minimal membrane conjecture.

demonstrate that the universal properties implied by the MMP are encoded in the growth exponents of the entanglement fluctuations, as summarized in the table of Fig. 1. We also provide robust numerical evidence that the upper critical dimension is $d = d_c = 4$, beyond which the fluctuations become Gaussian.

The minimal membrane conjecture for entanglement growth.—We are interested in noisy quantum dynamics that arises from the randomness of a quantum circuit or that stems from a Hamiltonian evolution with time-dependent fluctuations. Here, we focus on the entanglement dynamics of a random unitary circuit on the lattice Λ. We start from a weakly entangled state $|\Psi_0\rangle$ and apply random two-body gates acting on neighboring sites and on-site random gates that are uncorrelated in space and time (see below for the details of the circuit). The resulting evolved state after the application of t layers $\hat{\mathcal{U}}_k$ of the quantum circuit reads $|\Psi_t\rangle = \hat{\mathcal{U}}_t, \ldots, \hat{\mathcal{U}}_1 |\Psi_0\rangle$. We quantify its entanglement via the von Neumann entropy defined for a bipartition $A \cup B$ of the lattice Λ as $S(A, t) \equiv -\mathrm{tr}(\rho_A \log_2 \rho_A)$ with $\rho_A = \mathrm{tr}_B(|\Psi_t\rangle\langle\Psi_t|)$.

According to the MMP of [63], entanglement evolution under such a noisy unitary dynamics maps to the well-studied problem of an elastic manifold pinned by point disorder [66,67,72]. In a nutshell, the latter is the problem of a d-dimensional interface in a $(d+1)$-dimensional disordered medium, with impurities uncorrelated along both the growth (Euclidean time) direction and its orthogonal directions. It describes a wide range of phenomena, including domain walls in magnets, vortex lattices in superconductors, or contact lines at depinning transitions [69]. The pinned membrane is characterized by two universal exponents θ and ζ, which, for a manifold of linear size ℓ, govern the fluctuations of energy ($\propto \ell^\theta$) and of membrane width ($\propto \ell^\zeta$). They are related by a hyperscaling relation $\theta = 2\zeta + d - 2$ [72]. Renormalization group and numerical simulations predict $\zeta \simeq 0.21(4-d)$ and $\theta = 0.84(3)$ [$\theta = 1.45(4)$] in $d = 2$ ($d = 3$) [70], while the fluctuations become Gaussian at the upper critical dimension $d_c = 4$ [72].

The MMP states that the entanglement entropy $S(A, t)$ at time (circuit depth) t scales, in the coarse-grained limit, proportionally to the energy of a d-dimensional membrane immersed in a $(d+1)$-dimensional disordered medium. In particular, the entanglement entropy is divided into the sum of a leading nonfluctuating term proportional to the surface of the membrane $t \times |\partial A|$ (where $|.|$ denotes the size of a subsystem) (cf. [11]) and a subleading term which encompasses energy of the fluctuations of the membrane. This, for $t \lesssim L$ and $x = L/2$, results in [63]

$$S(L/2, t) = \tilde{v} t L^{d-1} + \tilde{b} t^{\theta+1-d} L^{d-1} \chi(t), \tag{1}$$

where $\chi(t)$ is a stochastic variable, and $\tilde{v}, \tilde{b}$ are constants depending on the microscopic details of the model. The form of Eq. (1) is obtained by dividing the membrane into $(L/t)^{d-1}$ boxes of linear size $\ell = t$, each contributing, respectively, a factor ℓ^d and ℓ^θ to the leading and the subleading terms. For $d \geq 2$, the subleading term in Eq. (1) is suppressed in time. Hence, to simplify the study of the fluctuations of entanglement entropy, we consider

$$w(L/2, t) \equiv \sqrt{\langle S(L/2, t)^2\rangle - \langle S(L/2, t)\rangle^2} \propto L^{(d-1)/2} t^\beta, \tag{2}$$

where $\langle \circ \rangle$ is the average over circuit realizations. The growth exponent $\beta = \theta + (1-d)/2$ arises from the contributions ℓ^θ of distant boxes that are statistically independent and add up incoherently, resulting in fluctuations that scale with the square root $(L/t)^{(d-1)/2}$ of the number of boxes. To probe the spatial structure of the noisy entanglement growth, we consider an equal-time correlator

$$G(r, t) \equiv \sqrt{\langle [S(x, t) - S(x+r, t)]^2\rangle} = r^{\beta/\zeta} g\left(\frac{r}{t^\zeta}\right), \tag{3}$$

where g is a scaling function, the dependence on r/t^ζ arises due to the emerging length scale ℓ^ζ characterizing the spatial fluctuations of the membrane, and $r^{\beta/\zeta}$ is the short-range behavior of the equal-time correlator for the pinned membrane problem. The MMP was tested in $(1+1)$-dimensional random circuits [63], yielding the KPZ exponents $\theta = 1/3$ and $\zeta = 2/3$ [77]. In the following, we argue that (2) and (3) also describe noisy entanglement growth in higher-dimensional systems.

Numerical results.—Assuming the MMP, the above discussion is relevant for any choice of the unitary ensemble of the random gates. Nevertheless, numerical simulations of generic (e.g., Haar) random circuits require computational resources that scale exponentially with the number $N \equiv |\Lambda|$ of qubits. Therefore, this Letter resorts to Clifford circuits, whose dynamics are efficiently simulable via the Gottesmann-Knill theorem [78–81].

A pure stabilizer state $|\Psi\rangle$ is determined by N independent Pauli strings $\hat{P}_\mu$ as $|\Psi\rangle\langle\Psi| = \prod_{\mu=1}^N (\hat{\mathbb{1}} + \hat{P}_\mu)/2$ [79]. Denoting the Pauli matrices at site $\mathbf{i}$ by $\hat{X}_\mathbf{i}, \hat{Y}_\mathbf{i}, \hat{Z}_\mathbf{i}$, we parametrize the Pauli strings as $\hat{P}_\mu = e^{i\phi^\mu} \prod_{\mathbf{i}\in\Lambda} \hat{X}_\mathbf{i}^{n_\mathbf{i}^\mu} \hat{Z}_\mathbf{i}^{m_\mathbf{i}^\mu}$ with $n_\mathbf{i}^\mu, m_\mathbf{i}^\mu, \phi^\mu \in \{0, 1\}$. Clifford gates are defined as unitary operators that map a Pauli string into a single Pauli string. Thus, for our Clifford circuit $|\Psi_t\rangle\langle\Psi_t| = \hat{\mathcal{U}}_t |\Psi_{t-1}\rangle\langle\Psi_{t-1}| \hat{\mathcal{U}}_t^\dagger = \prod_{\mu=1}^N [\hat{\mathbb{1}} + \hat{\mathcal{U}}_t \hat{P}_\mu(t-1) \times \hat{\mathcal{U}}_t^\dagger]/2 = \prod_{\mu=1}^N [\hat{\mathbb{1}} + \hat{P}_\mu(t)]/2$, where $P_\mu(t)$ are the Pauli strings determining $|\Psi_t\rangle$. Hence, the state's dynamics is fully encoded in the $(2N+1)N$ time-dependent coefficients $\phi^\mu(t), n_\mathbf{i}^\mu(t), m_\mathbf{i}^\mu(t)$. Consequently, the unitary evolution under Clifford circuits is simulable in resources scaling polynomially with N. Furthermore, the

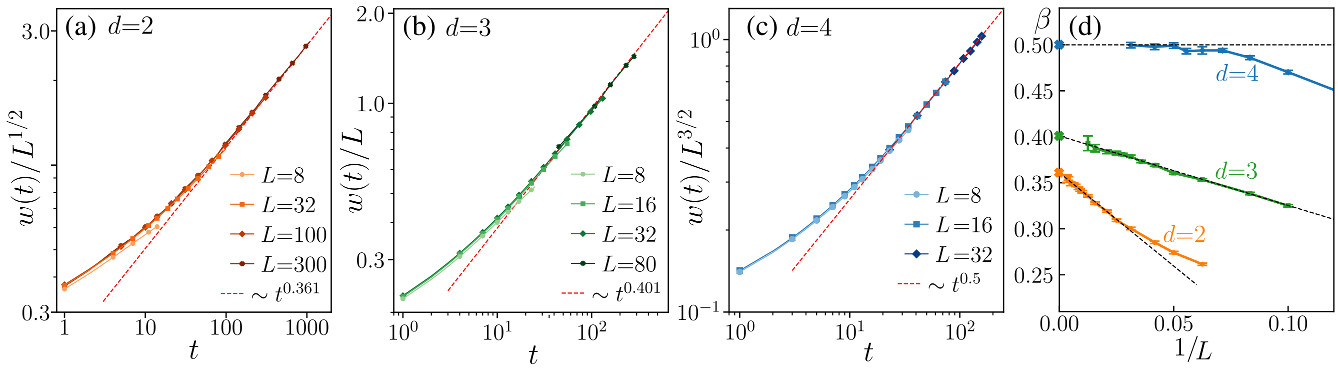

FIG. 2. Entanglement entropy fluctuations $w(t)$ in $(d+1)$-dimensional random Clifford circuits. The $w(t)$ rescaled by $L^{[(d-1)/2]}$ for system size L is shown as a function of the time t in panels (a), (b), and (c), respectively for $d=2, 3, 4$. The dashed lines denote power-law dependences t^{β} where β are the extrapolated exponents (see text). The values of β_L are shown as functions of $1/L$ in (d) for $d=2$, 3, 4, and the extrapolation to the $L\to\infty$ limit is performed with a first-order polynomial in $1/L$, yielding $\beta=0.361(6)$, $\beta=0.401(9)$, $\beta=0.500(5)$, respectively, for $d=2$, 3, 4.

entanglement entropy of stabilizer states is efficiently computable as $S(A,t)=r_A(t)-N_A$, where $N_A=|A|$ is the number of the qubits in A, and $r_A(t)=rk_{\mathbb{F}_2}M_A(t)$ is the rank over the Galois field $\mathbb{F}_2$ [82] of the $N\times(2N_A)$ matrix $M_A(t)=[n^{\mu}_{\mathbf{i}}(t), m^{\mu}_{\mathbf{i}}(t)]_{\mathbf{i}\in A,\mu=1,\ldots,N}$ [83,84]. Earlier calculations of $S(A,t)$ in the literature were based on standard Jordan-Gauss elimination, with complexity $O(N^3)$. Here, we employ an asymptotically fast rank-revealing algorithm with complexity $O(N^3/\log_2 N)$ [85,86]. We combine an efficient implementation of this algorithm [87] with a state-of-the-art STIM [88] library to perform large-scale computations for systems of up to $N=131\,072$ qubits. The $S(A,t)$ calculation for the largest considered N is around 2 orders of magnitude faster than a naive implementation of Jordan-Gauss elimination in STIM.

A layer of our circuit $\hat{\mathcal{U}}_k=(\prod_{\langle\mathbf{i},\mathbf{j}\rangle\in I^{(2)}_t}\hat{U}_{\mathbf{i},\mathbf{j}})\prod_{\mathbf{i}\in I^{(1)}_t}\hat{U}_{\mathbf{i}}$ comprises random two-body gates $\hat{U}_{\mathbf{i},\mathbf{j}}$ acting on neighboring sites $\mathbf{i}$, $\mathbf{j}$ and on-site random gates $\hat{U}_{\mathbf{i}}$ applied to random sites belonging to the sets of indices $I^{(1,2)}_t$. Here, $I^{(1)}_t$ is a set of $N/2$ randomly chosen sites, and $\hat{U}_{\mathbf{i}}$ are selected randomly, with equal probability, to be either Hadamard $\hat{H}_{\mathbf{i}}=(\hat{X}_{\mathbf{i}}+\hat{Z}_{\mathbf{i}})/\sqrt{2}$ or phase $\sqrt{\hat{Z}_{\mathbf{i}}}$ gates [89].

Instead, $I^{(2)}_t$ is a set of $N/4$ pairs of nearest-neighboring sites $\langle\mathbf{i},\mathbf{j}\rangle$ where $\mathbf{i}$ is picked randomly with uniform distribution on Λ, and $\mathbf{j}=\mathbf{i}+\mathbf{e}_u$ where $\mathbf{e}_u$ is a versor in a randomly chosen direction $u=1,\ldots,d$. The gates $\hat{U}_{\mathbf{i},\mathbf{j}}$ are chosen with equal probability between controlled-NOT (CNOT) gates [79] controlled by the left or the right qubit [90]. The initial state is $|\Psi_0\rangle=\otimes_{\mathbf{i}\in\Lambda}|0_{\mathbf{i}}\rangle$, where $\hat{Z}_{\mathbf{i}}|1_{\mathbf{i}}\rangle=|1_{\mathbf{i}}\rangle$, $\hat{Z}_{\mathbf{i}}|0_{\mathbf{i}}\rangle=-|0_{\mathbf{i}}\rangle$ [91]. We checked, but did not report here, that other low-entangled initial states yield quantitatively consistent results.

First, we consider the fluctuations $w(t)\equiv w(L/2,t)$ of the entanglement entropy; cf. Eq. (2). Our findings are summarized in Fig. 2, where we let the system evolve to time $t=4L$. For a fixed system size L, the time evolution of $w(t)$ can be parametrized by a power-law dependence $w(t)\sim t^{\beta(t)}$, with a flowing exponent $\beta(t)$ that increases with t until $t=t_{\mathrm{sat}}$. At t_{sat}, which is approximately equal to $4L$ for our circuit architecture, the entropy growth saturates due to the finite system size, and entropy fluctuations are strongly suppressed (data in the regime $t>t_{\mathrm{sat}}$ are not shown in Fig. 2). Moreover, our numerical results indicate that $\beta(t)$ converges, at sufficiently large t and L, to a time-independent exponent β, consistent with the behavior conjectured in Eq. (2). In order to obtain the exponent β that describes the growth of $w(t)$ in the asymptotic limit of large t and L, we employ the following extrapolation scheme. Fixing L, we fit $w(t)$ with a power-law t^{β_L} in a time interval $[t_1,t_2]$. We maximize the exponent β_L over choices of t_1 and t_2 such that $t_2-t_1>\Delta t$, where Δt is a constant which assures that the fitting interval is sufficiently long (we put $\Delta t=40$ for $d=2$, 3 and $\Delta t=10$ for $d=4$) and $t_2<t_{\mathrm{sat}}$. In this way, given the monotonic increase of $\beta(t)$ with time, β_L estimates, at a fixed L, the asymptotic exponent β. Finally, we extrapolate β_L to the thermodynamic limit $L\to\infty$ using a first-order polynomial in $1/L$ [see Fig. 2(d)], obtaining, respectively, $\beta=0.361(6)$, $\beta=0.401(9)$, and $\beta=0.500(5)$ for $d=2$, 3, 4 in agreement with the pinned membrane exponents (cf. table in Fig. 1), where the values of $\theta=\beta-(1-d)/2$ are presented.

Furthermore, we consider the spatiotemporal fluctuations $G(r,t)$; cf. Eq. (3). We fix the system sizes to be equal to $L=360$ and $L=64$ for $d=2$ and $d=3$, respectively, and study the growth of the fluctuations varying r and t. [The $d=2$ case is presented in Fig. 3(a), while the result for $d=3$ is qualitatively similar and is not shown here.] The behavior of $G(r,t)$ can be analyzed with the hypothesis (3), where the exponents β and ζ are obtained by finding an optimal collapse of results for different circuit depths t. To perform the analysis in an unbiased fashion, we

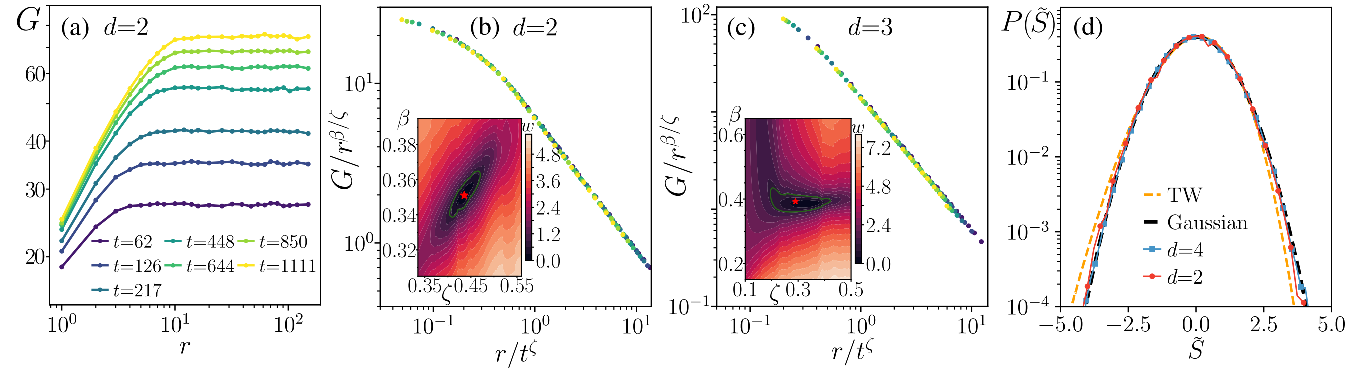

FIG. 3. The correlator $G(r,t)$ is plotted in (a) as a function of r for various times t for a $d=2$ circuit and $L=360$. The data for different times t are collapsed according to (3) in (b), yielding the exponents $\beta=0.351(12)$, $\zeta=0.435(33)$ with the cost function $C(\beta,\gamma)$ shown in the inset. (c) The same for $d=3$, the optimal exponents are $\beta=0.39(3)$, $\zeta=0.3(1)$. Distribution of $\tilde{S}$ at time $t=L$ is shown in (d) for $d=2$, 4 and compared with the Gaussian and standardized Tracy-Widom distributions.

consider both β and ζ as unknown parameters, and optimize the cost function $C(\beta,\zeta)=\sum_{i=2}^{n-1}c(x_i,y_i,d_i)$ with $x_i=(r_i/t_i^{\zeta})$, $y_i=G(r_i,t_i)/r_i^{\beta/\zeta}$, and $d_i=\sigma(y_i)$, respectively, the hyperparameters, data, and standard deviations. The indices $i=0,\ldots,\mathcal{N}_{\mathrm{data}}$ are ordered such that $x_i<x_j$ when $i<j$ [92–94], and the density $c(x_i,y_i,d_i)=(y-\bar{y})^2/\Delta$ depends on $\bar{y}=[(x_{i+1}-x_i)y_{i-1}-(x_{i-1}-x_i)y_{i+1}]/(x_{i+1}-x_{i-1})$ and on

$$\Delta=d_i^2+\left(\frac{x_{i+1}-x_i}{x_{i+1}-x_{i-1}}d_{i-1}\right)^2+\left(\frac{x_{i-1}-x_i}{x_{i+1}-x_{i-1}}d_{i+1}\right)^2.$$

The optimal growth exponents are obtained via minimization $\beta^\star,\zeta^\star=\arg\min C(\beta,\zeta)$, and lead to the data collapses in Figs. 3(b) and 3(c) for $d=2$ and $d=3$, respectively. In the insets, we present the cost function landscape $C(\beta,\zeta)$. In $d=2$, our estimates $\beta=0.351(12)$ and $\zeta=0.435(33)$ correspond to a relatively narrow dip in $C(\beta,\zeta)$ leading to exponents compatible with the pinned membrane ones. In $d=3$, the cost function [cf. Fig. 3(c) inset] possesses a wide minimum, which leads to larger error bars on the estimates $\beta=0.39(3)$ and $\zeta=0.3(1)$. Still, these values are compatible with the membrane predictions; cf. table in Fig. 1.

Lastly, we study the distribution of the rescaled entanglement entropy $\tilde{S}\equiv[S(L/2,t)-\langle S(L/2,t)\rangle]/w(L/2,t)$. For $d=1$, $\tilde{S}$ follows the centralized Tracy-Widom (TW) distribution [63], whereas, for $d=d_c=4$, the system is expected to reach a Gaussian distribution [69,72]. For $d=2$, 3, the distribution is unknown but is expected to differ from the TW and Gaussian ones. Our results for $d=2$, 4 are given in Fig. 3(d) at $t=L$ for $L=320$ and $L=32$, respectively. We see that both distributions are closer to the Gaussian fit than to the TW. To quantify the closeness to Gaussianity, we investigate the skewness κ_3 of $P(\tilde{S})$. The TW distribution relevant for the $d=1$ case yields $\kappa_3\approx0.2241$, while we find that the $d=2$ distribution has $\kappa_3=0.07(1)$, showing that the distribution is non-Gaussian. For $d=3$, we obtain that $\kappa_3=0.004(3)$. Hence, while the distribution $P(\tilde{S})$ approaches the Gaussian distribution with increasing system dimension, we still observe mild deviations from Gaussianity at the level of the $P(\tilde{S})$ for $d=3$, consistent with the nonmean field values of the exponents θ and ζ. Instead, for $d=4$, the numerically obtained $P(\tilde{S})$ is indistinguishable from Gaussian, and we find $\kappa_3=0.000(4)$ confirming the MMP prediction for the upper critical dimension.

Conclusions and outlook.—This Letter investigates the structural properties of entanglement propagation in $(d+1)$-dimensional random unitary circuits encoded in the fluctuations and distribution of the entanglement entropy. Focusing on Clifford circuits, we compute the growth exponents θ and ζ for $d\le4$ with high accuracy. We find they are compatible with the corresponding exponents governing the fluctuations of a membrane pinned by disorder in an elastic manifold; cf. table in Fig. 1. Furthermore, at $d=4$, the entanglement fluctuations become Gaussian, in accordance with the upper critical dimension of membranes pinned by disorder in $d+1$ manifolds. Overall, our findings demonstrate the effectiveness of the recently proposed MMP in capturing the structure of entanglement dynamics [63].

Beyond numerical considerations, the entanglement growth may be analytically treatable even in higher dimensions [64,65,95] in certain limits (e.g., of large local Hilbert space dimension). At the same time, it would be interesting to investigate the properties of the volume-law phase in $(d+1)$-dimensional monitored systems [96–116] and long-range systems [117–121]. While recent works for $(1+1)D$ circuits revealed a rich structure related to polymer defects [122–125], the case of higher dimensions has been left essentially unexplored. A first step in $(d+1)$ dimensions was recently presented by Ref. [126] for interacting Majorana circuits, where nontrivial subleading corrections due to the topological nature of the system were found. A possible future direction is to relate the $L \ln L$ subleading behavior to Fermi surface corrections in the spirit of the Widom conjecture [127], or to the statistical mechanics of loop models [128–131].

We thank A. Nahum and T. Zhou for discussions. We acknowledge the workshop "Dynamical Foundation of Many-Body Quantum Chaos" at Institute Pascal (Orsay, France) for hosting P. S. and X. T. during the finalizing stage of this Letter's writing. X. T. and M. S. acknowledge support from the ANR grant NonEQuMat (Grant No. ANR-19-CE47-0001) and computational resources on the Coll e de France IPH cluster. P. S. and M. L. acknowledge ERC AdG NOQIA; MCIN/AEI (PGC2018-0910.13039/501100011033, CEX2019-000910-S/10.13039/501100011033, Plan National FIDEUA PID2019-106901GB-I00, Plan National STAMEENA PID2022-139099NB-I00 project funded by MCIN/AEI/10.13039/501100011033 and by the "European Union NextGenerationEU/PRTR"; (PRTR-C17.I1), FPI); QUANTERA MAQS PCI2019-111828-2); QUANTERA DYNAMITE PCI2022-132919 (QuantERA II Programme co-funded by European Union's Horizon 2020 program under Grant Agreement No. 101017733), Ministry of Economic Affairs and Digital Transformation of the Spanish Government through the QUANTUM ENIA project call—Quantum Spain project, and by the European Union through the Recovery, Transformation, and Resilience Plan—NextGenerationEU within the framework of the Digital Spain 2026 Agenda; Fundació Cellex; Fundació Mir-Puig; Generalitat de Catalunya (European Social Fund FEDER and CERCA program, AGAUR Grant No. 2021 SGR 01452, QuantumCAT\U16-011424, co-funded by ERDF Operational Program of Catalonia 2014-2020); Barcelona Supercomputing Center MareNostrum (FI-2023-1-0013); EU Quantum Flagship (PASQuanS2.1, 101113690); EU Horizon 2020 FET-OPEN OPTOlogic (Grant No. 899794); EU Horizon Europe Program (Grant Agreement 101080086—NeQST), ICFO Internal "QuantumGaudi" project; European Union's Horizon 2020 program under the Marie Sklodowska-Curie Grant Agreement No. 847648; "La Caixa" Junior Leaders fellowships, La Caixa Foundation (ID 100010434): LCF/BQ/PR23/11980043. The views and opinions expressed are, however, those of the author(s) only and do not necessarily reflect those of the European Union, European Commission, European Climate, Infrastructure and Environment Executive Agency or any other granting authority. Neither the European Union nor any granting authority can be held responsible for them.

[1] N. Laflorencie, Phys. Rep. **646**, 1 (2016).
[2] L. Amico, R. Fazio, A. Osterloh, and V. Vedral, Rev. Mod. Phys. **80**, 517 (2008).
[3] A. C. Potter and R. Vasseur, in *Quantum Science and Technology* (Springer International Publishing, New York, 2022), pp. 211–249.
[4] J. M. Deutsch, Phys. Rev. A **43**, 2046 (1991).
[5] M. Srednicki, Phys. Rev. E **50**, 888 (1994).
[6] S. Pappalardi, L. Foini, and J. Kurchan, Phys. Rev. Lett. **129**, 170603 (2022).
[7] C. Gogolin and J. Eisert, Rep. Prog. Phys. **79**, 056001 (2016).
[8] L. D'Alessio, Y. Kafri, A. Polkovnikov, and M. Rigol, Adv. Phys. **65**, 239 (2016).
[9] L. Zhang, H. Kim, and D. A. Huse, Phys. Rev. E **91**, 062128 (2015).
[10] W. W. Ho and D. A. Abanin, Phys. Rev. B **95**, 094302 (2017).
[11] M. Žnidarič, Commun. Phys. **3**, 100 (2020).
[12] G. De Chiara, S. Montangero, P. Calabrese, and R. Fazio, J. Stat. Mech. (2006) P03001.
[13] M. Žnidarič, T. Prosen, and P. Prelovšek, Phys. Rev. B **77**, 064426 (2008).
[14] J. H. Bardarson, F. Pollmann, and J. E. Moore, Phys. Rev. Lett. **109**, 017202 (2012).
[15] D. A. Huse, R. Nandkishore, and V. Oganesyan, Phys. Rev. B **90**, 174202 (2014).
[16] D. A. Abanin, E. Altman, I. Bloch, and M. Serbyn, Rev. Mod. Phys. **91**, 021001 (2019).
[17] M. Serbyn, Z. Papić, and D. A. Abanin, Phys. Rev. Lett. **110**, 260601 (2013).
[18] R. Nandkishore and D. A. Huse, Annu. Rev. Condens. Matter Phys. **6**, 15 (2015).
[19] F. Alet and N. Laflorencie, C.R. Phys. **19**, 498 (2018).
[20] P. Sierant and J. Zakrzewski, Phys. Rev. B **105**, 224203 (2022).
[21] T. Farshi, D. Toniolo, C. E. González-Guillén, A. M. Alhambra, and L. Masanes, J. Math. Phys. (N.Y.) **63**, 032201 (2022).
[22] T. Farshi, J. Richter, D. Toniolo, A. Pal, and L. Masanes, PRX Quantum **4**, 030302 (2023).
[23] J. Schachenmayer, B. P. Lanyon, C. F. Roos, and A. J. Daley, Phys. Rev. X **3**, 031015 (2013).
[24] P. Hauke and L. Tagliacozzo, Phys. Rev. Lett. **111**, 207202 (2013).
[25] A. Lerose and S. Pappalardi, Phys. Rev. Res. **2**, 012041(R) (2020).
[26] A. Lerose and S. Pappalardi, Phys. Rev. A **102**, 032404 (2020).
[27] S. Pappalardi, A. Russomanno, B. Žunkovič, F. Iemini, A. Silva, and R. Fazio, Phys. Rev. B **98**, 134303 (2018).
[28] J. Abajo-Arrastia, J. Aparício, and E. López, J. High Energy Phys. 11 (2010) 149.
[29] V. E. Hubeny, M. Rangamani, and T. Takayanagi, J. High Energy Phys. 07 (2007) 062.
[30] H. Liu and S. J. Suh, Phys. Rev. D **89**, 066012 (2014).
[31] H. Liu and S. J. Suh, Phys. Rev. Lett. **112**, 011601 (2014).
[32] D. A. Roberts, D. Stanford, and L. Susskind, J. High Energy Phys. 03 (2015) 051.
[33] B. Swingle, Phys. Rev. D **86**, 065007 (2012).
[34] P. Hayden and J. Preskill, J. High Energy Phys. 09 (2007) 120.

[35] Y. Sekino and L. Susskind, J. High Energy Phys. 10 (2008) 065.
[36] P. Calabrese and J. Cardy, J. Stat. Mech. (2004) P06002.
[37] P. Calabrese and J. Cardy, J. Stat. Mech. (2005) P04010.
[38] P. Calabrese and J. Cardy, J. Phys. A **42**, 504005 (2009).
[39] P. Calabrese and J. Cardy, J. Stat. Mech. (2016) 064003.
[40] C. T. Asplund, A. Bernamonti, F. Galli, and T. Hartman, J. High Energy Phys. 09 (2015) 110.
[41] M. Fagotti and P. Calabrese, Phys. Rev. A **78**, 010306(R) (2008).
[42] I. Peschel and V. Eisler, J. Phys. A **42**, 504003 (2009).
[43] V. Alba and P. Calabrese, Proc. Natl. Acad. Sci. U.S.A. **114**, 7947 (2017).
[44] V. Alba and P. Calabrese, SciPost Phys. **4**, 017 (2018).
[45] V. Alba and P. Calabrese, Europhys. Lett. **126**, 60001 (2019).
[46] V. Alba and P. Calabrese, Phys. Rev. B **100**, 115150 (2019).
[47] B. Bertini, P. Kos, and T. Prosen, Phys. Rev. X **9**, 021033 (2019).
[48] B. Bertini, P. Kos, and T. Prosen, SciPost Phys. **8**, 067 (2020).
[49] S. Gopalakrishnan and A. Lamacraft, Phys. Rev. B **100**, 064309 (2019).
[50] L. Piroli, B. Bertini, J. I. Cirac, and T. Prosen, Phys. Rev. B **101**, 094304 (2020).
[51] I. Reid and B. Bertini, Phys. Rev. B **104**, 014301 (2021).
[52] C. Jonay, V. Khemani, and M. Ippoliti, Phys. Rev. Res. **3**, 043046 (2021).
[53] B. Bertini, K. Klobas, and T.-C. Lu, Phys. Rev. Lett. **129**, 140503 (2022).
[54] H. Kim and D. A. Huse, Phys. Rev. Lett. **111**, 127205 (2013).
[55] A. M. Läuchli and C. Kollath, J. Stat. Mech. (2008) P05018.
[56] M. Rigol, V. Dunjko, and M. Olshanii, Nature (London) **452**, 854 (2008).
[57] R. Oliveira, O. C. O. Dahlsten, and M. B. Plenio, Phys. Rev. Lett. **98**, 130502 (2007).
[58] M. Žnidarič, Phys. Rev. A **78**, 032324 (2008).
[59] O. C. O. Dahlsten, C. Lupo, S. Mancini, and A. Serafini, J. Phys. A **47**, 363001 (2014).
[60] U. Schollwöck, Ann. Phys. (Amsterdam) **326**, 96 (2011).
[61] F. Verstraete, V. Murg, and J. Cirac, Adv. Phys. **57**, 143 (2008).
[62] M. P. Fisher, V. Khemani, A. Nahum, and S. Vijay, Annu. Rev. Condens. Matter Phys. **14**, 335 (2023).
[63] A. Nahum, J. Ruhman, S. Vijay, and J. Haah, Phys. Rev. X **7**, 031016 (2017).
[64] T. Zhou and A. Nahum, Phys. Rev. B **99**, 174205 (2019).
[65] T. Zhou and A. Nahum, Phys. Rev. X **10**, 031066 (2020).
[66] T. Nattermann, J. Phys. C **18**, 6661 (1985).
[67] D. A. Huse and C. L. Henley, Phys. Rev. Lett. **54**, 2708 (1985).
[68] E. E. Ferrero, L. Foini, T. Giamarchi, A. B. Kolton, and A. Rosso, Annu. Rev. Condens. Matter Phys. **12**, 111 (2021).
[69] K. J. Wiese, Rep. Prog. Phys. **85**, 086502 (2022).
[70] A. A. Middleton, Phys. Rev. E **52**, R3337 (1995).
[71] M. J. Alava and P. M. Duxbury, Phys. Rev. B **54**, 14990 (1996).
[72] D. S. Fisher, Phys. Rev. Lett. **56**, 1964 (1986).
[73] T. Halpin-Healy, Phys. Rev. A **42**, 711 (1990).
[74] P. Chauve, P. Le Doussal, and K. Wiese, Phys. Rev. Lett. **86**, 1785 (2001).
[75] P. Le Doussal, K. J. Wiese, and P. Chauve, Phys. Rev. E **69**, 026112 (2004).
[76] C. Husemann and K. J. Wiese, Nucl. Phys. **B932**, 589 (2018).
[77] M. Kardar, G. Parisi, and Y.-C. Zhang, Phys. Rev. Lett. **56**, 889 (1986).
[78] D. Gottesman, Phys. Rev. A **54**, 1862 (1996).
[79] M. A. Nielsen and I. L. Chuang, *Quantum Computation and Quantum Information* (Cambridge University Press, Cambridge, England, 2000).
[80] D. Gottesman, arXiv:quant-ph/9807006.
[81] S. Aaronson and D. Gottesman, Phys. Rev. A **70**, 052328 (2004).
[82] R. Lidl and H. Niederreiter, *Finite Fields* (Cambridge University Press, Cambridge, England, 1997), Vol. 20.
[83] A. Hamma, R. Ionicioiu, and P. Zanardi, Phys. Rev. A **71**, 022315 (2005).
[84] A. Hamma, R. Ionicioiu, and P. Zanardi, Phys. Lett. A **337**, 22 (2005).
[85] D. Andrén, L. Hellström, and K. Markström, Adv. Appl. Math. **39**, 428 (2007).
[86] M. R. Albrecht, G. V. Bard, and C. Pernet, arXiv:1111.6549.
[87] E. Bertolazzi and A. Rimoldi, J. Comput. Appl. Math. **260**, 519 (2014).
[88] C. Gidney, Quantum **5**, 497 (2021).
[89] In terms of the coefficients $n^\mu_{\mathbf{i}}(t), m^\mu_{\mathbf{i}}(t)$, $\hat{H}_{\mathbf{i}}$ acts trivially on $n^\mu_{\mathbf{j}}, m^\mu_{\mathbf{j}}$ with $\mathbf{j}\neq\mathbf{i}$, otherwise swaps $m^\mu_{\mathbf{i}}\leftrightarrow n^\mu_{\mathbf{i}}$. Similarly, $\sqrt{\hat{Z}_{\mathbf{i}}}$ act nontrivially only at site $\mathbf{i}$ as $m^\mu_{\mathbf{i}}\to(m^\mu_{\mathbf{i}}+n^\mu_{\mathbf{i}})$ mod 2.
[90] Namely, $\mathrm{CNOT}^L_{\mathbf{ij}}=[\hat{\mathbb{1}}+\hat{Z}_{\mathbf{i}}+(\hat{\mathbb{1}}-\hat{Z}_{\mathbf{i}})\hat{X}_{\mathbf{j}}]/2$ and $\mathrm{CNOT}^R_{\mathbf{ij}}=[\hat{\mathbb{1}}+\hat{Z}_{\mathbf{j}}+(\hat{\mathbb{1}}-\hat{Z}_{\mathbf{j}})\hat{X}_{\mathbf{i}}]/2$. In the stabilizer framework, the $\mathrm{CNOT}^L_{\mathbf{ij}}$ acts via $n^\mu_{\mathbf{j}}\to(n^\mu_{\mathbf{j}}+n^\mu_{\mathbf{i}})$ mod 2 and $m^\mu_{\mathbf{i}}\to(m^\mu_{\mathbf{i}}+m^\mu_{\mathbf{j}})$ mod 2 and trivially on the other sites. The $\mathrm{CNOT}^R_{\mathbf{ij}}$ acts similarly, with n and m roles exchanged.
[91] Enumerating the sites $\mathbf{i}\in\Lambda$ by $\mu(\mathbf{i})\in[1,|\Lambda|]$, the $|\Psi_0\rangle$ is specified by $\phi^{\mu(\mathbf{j})}=1$, $m^{\mu(\mathbf{j})}_{\mathbf{i}}=\delta_{\mathbf{i},\mathbf{j}}$, and $n^{\mu(\mathbf{j})}_{\mathbf{i}}=0$.
[92] N. Kawashima and N. Ito, J. Phys. Soc. Jpn. **62**, 435 (1993).
[93] A. Zabalo, M. J. Gullans, J. H. Wilson, S. Gopalakrishnan, D. A. Huse, and J. H. Pixley, Phys. Rev. B **101**, 060301(R) (2020).
[94] P. Sierant, M. Schirò, M. Lewenstein, and X. Turkeshi, Phys. Rev. B **106**, 214316 (2022).
[95] Y. Li, R. Vasseur, M. P. A. Fisher, and A. W. W. Ludwig, arXiv:2110.02988.
[96] Y. Li, X. Chen, and M. P. A. Fisher, Phys. Rev. B **98**, 205136 (2018).
[97] Y. Li, X. Chen, and M. P. A. Fisher, Phys. Rev. B **100**, 134306 (2019).
[98] B. Skinner, J. Ruhman, and A. Nahum, Phys. Rev. X **9**, 031009 (2019).

[99] A. Zabalo, M. J. Gullans, J. H. Wilson, R. Vasseur, A. W. W. Ludwig, S. Gopalakrishnan, D. A. Huse, and J. H. Pixley, Phys. Rev. Lett. **128**, 050602 (2022).
[100] P. Sierant and X. Turkeshi, Phys. Rev. Lett. **128**, 130605 (2022).
[101] Z. Weinstein, Y. Bao, and E. Altman, Phys. Rev. Lett. **129**, 080501 (2022).
[102] X. Turkeshi, R. Fazio, and M. Dalmonte, Phys. Rev. B **102**, 014315 (2020).
[103] X. Turkeshi, Phys. Rev. B **106**, 144313 (2022).
[104] Z. Weinstein, S. P. Kelly, J. Marino, and E. Altman, Phys. Rev. Lett. **131**, 220404 (2023).
[105] O. Lunt, J. Richter, and A. Pal, Quantum simulation using noisy unitary circuits and measurements, in *Entanglement in Spin Chains: From Theory to Quantum Technology Applications*, edited by A. Bayat, S. Bose, and H. Johannesson (Springer, Cham, 2022), pp. 251–284.
[106] S. P. Kelly, U. Poschinger, F. Schmidt-Kaler, M. P. A. Fisher, and J. Marino, arXiv:2210.11547.
[107] M. Szyniszewski, A. Romito, and H. Schomerus, Phys. Rev. B **100**, 064204 (2019).
[108] M. Szyniszewski, A. Romito, and H. Schomerus, Phys. Rev. Lett. **125**, 210602 (2020).
[109] S.-K. Jian, C. Liu, X. Chen, B. Swingle, and P. Zhang, Phys. Rev. Lett. **127**, 140601 (2021).
[110] J. Lopez-Piqueres, B. Ware, and R. Vasseur, Phys. Rev. B **102**, 064202 (2020).
[111] R. Vasseur, A. C. Potter, Y.-Z. You, and A. W. W. Ludwig, Phys. Rev. B **100**, 134203 (2019).
[112] C.-M. Jian, Y.-Z. You, R. Vasseur, and A. W. W. Ludwig, Phys. Rev. B **101**, 104302 (2020).
[113] A. Nahum, S. Roy, B. Skinner, and J. Ruhman, PRX Quantum **2**, 010352 (2021).
[114] A. Nahum and K. J. Wiese, Phys. Rev. B **108**, 104203 (2023).
[115] Y. Bao, S. Choi, and E. Altman, Phys. Rev. B **101**, 104301 (2020).
[116] S. Choi, Y. Bao, X.-L. Qi, and E. Altman, Phys. Rev. Lett. **125**, 030505 (2020).
[117] P. Sierant, G. Chiriacò, F. M. Surace, S. Sharma, X. Turkeshi, M. Dalmonte, R. Fazio, and G. Pagano, Quantum **6**, 638 (2022).
[118] J. Richter, O. Lunt, and A. Pal, Phys. Rev. Res. **5**, L012031 (2023).
[119] S. Sharma, X. Turkeshi, R. Fazio, and M. Dalmonte, SciPost Phys. Core **5**, 023 (2022).
[120] M. Block, Y. Bao, S. Choi, E. Altman, and N. Y. Yao, Phys. Rev. Lett. **128**, 010604 (2022).
[121] P. Sierant and X. Turkeshi, Phys. Rev. Lett. **130**, 120402 (2023).
[122] Y. Li and M. P. A. Fisher, Phys. Rev. B **103**, 104306 (2021).
[123] S. Vijay, arXiv:2005.03052.
[124] R. Fan, S. Vijay, A. Vishwanath, and Y.-Z. You, Phys. Rev. B **103**, 174309 (2021).
[125] Y. Li, S. Vijay, and M. P. A. Fisher, PRX Quantum **4**, 010331 (2023).
[126] G.-Y. Zhu, N. Tantivasadakarn, and S. Trebst, arXiv: 2303.17627.
[127] B. Swingle, Phys. Rev. Lett. **105**, 050502 (2010).
[128] A. Nahum, J. T. Chalker, P. Serna, M. Ortuño, and A. M. Somoza, Phys. Rev. Lett. **107**, 110601 (2011).
[129] A. Nahum, J. T. Chalker, P. Serna, M. Ortuño, and A. M. Somoza, Phys. Rev. X **5**, 041048 (2015).
[130] A. Nahum and B. Skinner, Phys. Rev. Res. **2**, 023288 (2020).
[131] K. Klocke and M. Buchhold, Phys. Rev. X **13**, 041028 (2023).